



(RESEARCH ARTICLE)



## Assessment of heavy metals in groundwater around Koppal Taluk, Koppal Dist. Karnataka by using multivariate analysis, metal pollution indices, and GIS technique

Ramesh <sup>1,2</sup> and Avinash Pandurang <sup>1,\*</sup>

<sup>1</sup> Department of Studies in Physics, Vijayanagara Sri Krishnadevaraya University, Ballari-583105, Karnataka, India.

<sup>2</sup> Department of Physics, Vijayanagar PU College, Hosapete - 583 201, Vijayanagara, Karnataka, India.

World Journal of Advanced Research and Reviews, 2025, 25(02), 2571-2590

Publication history: Received on 16 January 2025; revised on 24 February 2025; accepted on 27 February 2025

Article DOI: <https://doi.org/10.30574/wjarr.2025.25.2.0643>

### Abstract

Groundwater is a crucial environmental resource with significant economic and public health implications. This study investigates aquifer water quality in Koppal taluk, Karnataka, India, where agricultural practices, unregulated groundwater extraction, and industrial activities, particularly steel manufacturing, pose potential contamination risks. Given the local population's reliance on groundwater for daily needs, the presence of even trace amounts of toxic elements raises serious health concerns. Therefore, this research analyzes the concentrations of trace metals in the aquifers. Twenty-five groundwater samples were collected seasonally from December 2022 to November 2023 and analyzed using Inductively Coupled Plasma - Optical Emission Spectrometry. The Metal Index, Geo-accumulation Index, and Heavy Metal Pollution Index were employed to interpret the data. Multivariate statistical and integrated techniques were applied to examine interrelationships among variables. Factor analysis revealed that Zn, Fe, and Cu exhibited significant variability, accounting for 62.10%, 65.10%, and 77.17% of the total variance during the pre-monsoon, monsoon, and post-monsoon seasons. Cluster analysis indicated a common source for most of the detected trace metals. The spatial distribution of heavy metals was visualized using the Inverse Distance Weighting tool in ArcGIS 10.8. The observed heavy metal concentrations were within the permissible limit compared to the Bureau of Indian Standards IS:10500 and World Health Organization guidelines. HPI values below 100, MI values between 0 and 3, and  $I_{geo}$  values between 0 and 1 suggest that the groundwater is potable. This study offers valuable information for policymakers to develop effective regional pollution mitigation strategies.

**Keywords:** Groundwater; Heavy Metals; Koppal; Multivariate Statistic; Pollution Indices; Arcgis 10.8

### 1. Introduction

Groundwater is primarily consumed by many people worldwide, especially in semi-arid and arid places [1]. Dense metallic elements known as heavy metals may be toxic to mankind and other creatures of existence in small quantities. Nickel, arsenic, chromium, lead, aluminium, and cadmium are examples of frequently occurring heavy metals. Transportation, the processing of waste, and industrial and agricultural processes can all release these metals into the environment. They can accumulate in the food chain and contaminate the air, water, and soil. Humans can be exposed to toxins by breathing polluted air, ingesting contaminated food or water, or coming into close contact with contaminants or groundwater. Preventing heavy metal exposure is crucial for environmental and community health [2;3]. Their toxicity, persistence, and carcinogenic properties make their presence in groundwater a critical environmental issue demanding immediate action [4]. While some metals, including copper, iron, manganese, and nickel, are essential nutrients for bacteria and plants, others like chromium, lead, and cadmium are detrimental in specific amounts. The main source of hazardous metals in mining regions is smelting activities.

\* Corresponding author: Avinash Pandurang

The human body requires minimum amounts of certain heavy metals. For instance, adults can safely ingest 20–280 µg/day of Pb, while children can have 10–271 µg/day. Grownups should consume 15–50 µg of Cd daily, while children should consume 2–25 µg/day. Zn is required at 15 µg/day [5]. According to Virag and Gergely (2016) [6], the recommended daily intake of copper is 1.5–3 mg for adults and a dose of one mg for kids, Fe at 10–20 mg for adults and 7 mg for children, and Mn at 2–5 mg for adults and a maximum of 1.3 mg for children. However, too much consumption is detrimental to the human body [7]. Long-term health impacts of heavy metal-contaminated water have prompted numerous studies on groundwater contamination levels. In India, such pollution has known health consequences [8]. Similar concerns have been reported in China, where groundwater heavy metals pose carcinogenic and noncarcinogenic risks [9]. Research in Iran and Pakistan also highlights the adverse health effects of contaminated groundwater [10]. Heavy metals like Pb, Cr, Cd, Co, Ni, Cu, Mn, Fe, and Zn are of significant interest to researchers due to their health implications [11].

However, estimating geographic patterns of groundwater pollution by heavy metals is a crucial step. Based on the information gathered from sampling station borewells, several mapping techniques are used to predict heavy-metal levels in unsampled areas [12]. Inverse distance weighting (IDW) is a deterministic approach that is used to estimate unknown values by interpolating observed data at defined points. This technique may be applied to the mapping of various hydrochemical parameters in spatial [13;14]. The heavy metals index (MI) is a metric that takes into account the levels of various heavy metals in water samples [15]. MI is systematically computed to evaluate the drinkability of water assets. Another method of estimating the purity of water concerning toxic metals and their impact on the safety of humans is the Heavy Metal Pollution Index (HPI) [16]. Cluster analysis and factor analysis are valuable tools for summarizing large datasets, providing enhanced interpretation and a deeper understanding of water quality. These multivariate techniques facilitate the identification of underlying patterns and relationships among variables, offering insights into the complex interplay of factors influencing water quality [17;18]. Factor analysis and hierarchical cluster analysis are increasingly employed in environmental studies, particularly for the measurement and monitoring of heavy metals in environmental media. These multivariate statistical techniques offer valuable insights into complex datasets, facilitating the identification of pollution sources and the assessment of environmental risks [19-22; 15].

In this research study, authors selected this research area because of locating steel manufacturing industries, and consideration of variables such as traditional agricultural practices, irrigation methodologies, erratic rainfall patterns, indiscriminate groundwater extraction, and challenges including salinity, brackishness, and contamination from nitrate and fluoride along the principal river systems in Koppal Taluk [23], groundwater is the primary source of daily requirements for the living systems in these areas and till today no research carried out in this study area regarding trace metals levels and its seasonal dissimilarities. Therefore, this research undertakes a systematic analysis of Koppal Taluk's groundwater quality. This study is important since there isn't much information available about the concentrations of heavy metals in groundwater close to mining areas around Koppal Taluk. The primary objectives were to: 1) assessment of spatial distribution of heavy metals in Koppal taluk groundwater samples, 2) determination of critical pollutants and subsequent causes of pollution, and 3) assessment of degree of contamination with heavy metals. In summary, the study offers important information on medical concerns that residents may have and heavy metal toxicity in aquifer samples. The findings will help the community and incumbents put plans in place to reduce pollution and protect public health.

---

## 2. Materials and Methodology

### 2.1. Geology of study area

On August 25, 1997, the Raichur district in Karnataka was split into the Koppal district, which encompasses a geographical area of approximately 1375 square kilometers. Located in the former Hyderabad-Karnataka region, Koppal is characterized as one of the state's backward districts. The research region spans 75°54'0" E to 76°24'0" E in longitude and 15°6'0" N to 15°36'0" N in latitude.

Based on the census taken in 2011, the district has a cumulative population of 1,391,292 inhabitants in 588 inhabited and 40 empty settlements. The Koppal region's semi-arid climate results in sweltering summers and little precipitation, with a median rainfall per year of 572 mm. The majority of the year is pleasant and mild, except for the warmer months from March through mid-June, and with a rise in the intense summer of 45°C and lows as low as 16°C, December to January is the coldest month. Due to insufficient rainfall, the district experiences dry conditions for most of the year. The soil composition results from the weathering of parent rock, possibly hornblende, amphibolite, or biotite schist. Desolate plains covered with black soils define the district, including expanses of black cotton soil in granite, gneissic, and schistose terrains. Nalas are typically filled with loosely packed sand and kanker mixed with grey sandy soil.

The district's overall literacy rate is 55.02 percent, with 69% of men and 40% of women literate. This research study was carried out in Koppal Taluk, part of the Krishna basin. The primary streams draining the district are Maskinala, Ilkal-nadi, and Hirenala, falling under the Tungabhadra sub-basin and having ephemeral characteristics. The drainage system exhibits dendritic to subdendritic patterns, with drainage densities ranging from 1.4 to 7.0 km/sq.km. The Taluk's landscape is rocky, featuring sporadic granite hill mounds and shallow troughs. With a height of 622 meters above mean sea level, Ginigera has the highest peaks. Although the Taluk is mostly plain, the hydrogeology of the research area is primarily supported by gneisses, granites, and schists. Despite hard rocks not possessing fundamental porosity, secondary porosity and permeability arise via corrosion, cracking, ligaments, and geophysical features such as depressions and faults. This increased the wells' capability to release water [23].

## 2.2. Sample Collection and Analysis

Twenty-five distinct sampling sites were selected for monitoring the levels of trace metals in groundwater seasonally named as Pre-monsoon, Monsoon, and Post-monsoon over a period from December 2022 to November 2023 based on population density and usage of groundwater for their daily need as shown in Fig.1. The bottles were soaked in a 10% Nitric acid solution before sample collection to prevent chemical interactions with the sample elements. The collection of all samples followed the APHA 2000[24] guidelines, and immediately after collection, they were transferred to the laboratory in sterile, acid-washed polyethylene terephthalate (PET) bottles and kept in the freezer. Groundwater samples are analysed according to APHA standard guidelines.

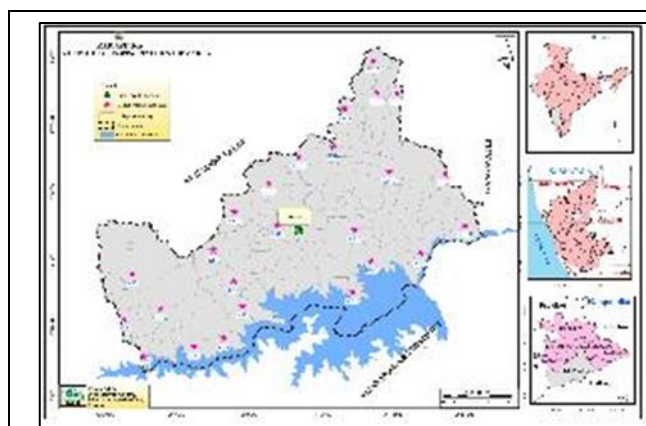


**Figure 1** Study area covering the Koppal Taluk, Koppal District



**Figure 2** Geology map of Koppal taluk, Koppal dist

The ICP source consists of a compressed stream of argon gas that was ionized by a radio frequency field, which frequently oscillates at 27.1 MHz. A quartz torch confines and maintains the plasma and a water-cooled coil enclosing it inductively links this field to the ionized gas. A specimen of the spray is created in a suitable nebulizer and spray chamber, and then it is fed into the plasma using a feeding tube inside the torch. The plasma's high temperature effectively stimulates atomic emission. ICP provides effective excitation, which accounts for many elements' low detection limits [25].

## 2.3. Quality Assurance (QA)/Quality Control (QC)

Double distilled water was used to prepare reagent solutions and reagent blanks. A linear curve was created by aspirating five distinct linear concentration standards—ranging from 1.0 ppb to 500.0 ppb—into the ICP-OES apparatus before sample analysis. When standard curves were prepared, those metals with acceptable linear graphs and correlation coefficients greater than 0.999 were noted. The instrument should be warmed up for 30 minutes. As instructed by the manufacturer, execute optical alignment and calibrate polychromators using standards and a blank.

Each sample run should begin with a calibration blank analysis, followed by a method blank analysis. Alternate between sample analysis and calibration blank analysis, rinsing with dilute acid for at least 60 seconds between samples and blanks. Before beginning waveform convergence, aspirate every reference or blank for 15 seconds after it reaches the plasma. Then, flush with a calibration blank or corresponding solution for a minimum of 60 seconds following each standard. Analyze the instrument check standard to ensure concentration values do not deviate by more than  $\pm 5\%$ . This should be done every five samples to monitor for significant instrument drift. After every analysis, all equipment was cleaned using suggested rinsing solutions for improved accuracy [25].

### 3. Methodology

#### 3.1. Pollution Indices:

##### 3.1.1. Heavy Metal Pollution Index (HPI):

The heavy metals pollution index serves as a digital methodology for identifying groundwater contamination, as it consolidates diverse characteristics into a singular metric, which is subsequently assessed against a predetermined threshold value to analyze pollutant concentration. Groundwater is categorized into three zones: minimal (less than 90), moderate (90-180), and elevated (over 180) based on HPI values [26;27]. With the heavy metal pollution index (HPI), the World Health Organization (WHO) established quantifiable thresholds for both the standard permissible figures ( $S_i$ ) and the ideal figures ( $I_i$ ) utilized in this study. The highest allowable level of drinking water, designated as the maximum permitted quantity, is defined as  $S_i$  when alternative water sources are unavailable. Conversely, the ideal maximum value ( $I_i$ ) denotes the regulatory limit for drinking water concerning the same parameter [28].

The conventional pollution index pertaining to HPI concentrations in groundwater typically registers at 100, which has been derived utilizing the equation delineated below.

$$HPI = \frac{\sum_{i=1}^n [W_i * Q_i]}{\sum_{i=1}^n (W_i)} \text{ -----(1)}$$

where  $W_i$  denotes the Unit weight associated with the  $i^{\text{th}}$  parameter,  $Q_i$  signifies the Sub index corresponding to the  $i^{\text{th}}$  parameter.

##### Metal Index (MI):

The Heavy Metal index methodology, as proposed by Tamasi and Cini in 2004, [29] represents one of the fundamental techniques for assessing heavy metal indices and is employed to ascertain the concentration and prevalence of trace metals in groundwater samples. This methodology provides a rapid assessment of the overall condition of groundwater status of heavy metal pollution. This index method was expressed as follows:

$$MI = \frac{\sum_{i=1}^n C_i}{MAC_i} \text{ -----(2)}$$

MI represents the Metal Index, while  $C_i$  denotes the average concentration of the  $i^{\text{th}}$  trace metals present in the analyzed sample.  $MAC_i$  signifies the maximum permissible concentration of the  $i^{\text{th}}$  heavy metals. The subsequent Table 1 provides the classification of groundwater quality.

**Table 1** Classification of MI index for groundwater quality.

Class	Property/Characteristics	MI value
I	Very Pure	<0.3
II	Pure	0.3-1
III	Slightly affected	1-2
IV	moderately affected	2-4
V	strongly affected	4-6
VI	Seriously affected	>6

3.1.2. Geo accumulation index ( $I_{geo}$ )

$I_{geo}$ , developed by G. Mullar in 1969, [30] quantifies the presence of harmful metal concentrations within sediments. It elucidates the origins of pollution as well as the contributions from lithogenic sources to the toxic metal concentrations in soil.  $I_{geo}$  consolidates unrefined data into a singular index metric, embodying trace metal concentrations relevant to environmental studies. This index is dedicated to a specific heavy metal and categorizes it into seven distinct classes, ranging from 0 to 6 as shown in Table 2. A positive  $I_{geo}$  value denotes a contribution from anthropogenic activities.

$I_{geo}$  value is calculated using the below formula:

$$I_{geo} = \text{Log}_2 \frac{C_n}{1.5 \cdot B_n} \text{ -----(3)}$$

$C_n$  - Denotes the concentration of the  $i^{\text{th}}$  heavy metal within the sample, 1.5 - A constant accounting for potential fluctuations in background data resulting from lithological differences.  $B_n$  - Represents the core geochemical reference point for the  $i^{\text{th}}$  heavy metal present in the sample.

**Table 2** Classification of  $I_{geo}$  index

Index class	$I_{geo}$ value	level of pollution
0	$I_{geo} < 0$	pure
1	$0 < I_{geo} < 1$	pure to modestly polluted
2	$1 < I_{geo} < 2$	modestly polluted
3	$2 < I_{geo} < 3$	Modestly to heavily polluted
4	$3 < I_{geo} < 4$	Heavy polluted
5	$4 < I_{geo} < 5$	Heavy polluted to extremely polluted
6	$5 < I_{geo} < 6$	extremely polluted

3.2. Spatial Distribution (Inverse Distance Weighting IDW) Using ArcGIS 10.8:

IDW, a deterministic interpolation method that combines multivariate analysis of statistics with GIS, is often used in groundwater research. The inverse distance weighting approach theoretically justifies giving nearby locations a larger weight compared to remote ones [31]. IDW calculations were performed on adjacent recorded regions in this work, suggesting that the identified locations function autonomously of one another [32].

$$Z = \frac{\sum_{i=1}^n \frac{Z_i}{d_i^p}}{\sum_{i=1}^n \frac{1}{d_i^p}} \text{ -----(4)}$$

where  $n$  is the total number of values acquired by interpolation,  $d_i$  is the distance between the calculated value  $Z_i$  and the interpolated value  $Z$ ,  $p$  is the weighting power, and  $Z$  is the projected amount at an interpolated location.

It is an extensive computer-based method crucial for pollution research and water resource management. It also recognizes hydrochemical properties and their applicability for various uses. This geographic analysis technique helps to understand unknown data from known information. Based on the results, the concentrations of the heavy metals under study were regionally distributed in maps using the Inverse Distance weighted (IDW) tool in ArcGIS 10.8 software [33].

A thematic contour is generated by controlling the relevance of known locations based on their distance from the output point and determining cell values using a weighted collection of sample points. A conversion tool transforms the polygon into a raster dataset, and GIS determines the range of the created maps [34], as shown in Fig 3.

### 3.3. Pearson's Correlation matrix

The sample Pearson correlation coefficient is another name for Pearson's correlation coefficient, which is represented by  $r$  when applied to a sample. The mathematical equation for  $r$  can be derived by substituting sample-based estimates of covariance and variances into the following equation:

$$r = \frac{n\sum xy - x\sum y}{\sqrt{[n\sum x^2 - (\sum x)^2][n\sum y^2 - (\sum y)^2]}} \dots \dots \dots (5)$$

where the quantities from which the correlation coefficient has to be determined are  $x$  and  $y$ . The standard deviation values of  $x$  and  $y$  are denoted by  $X$  and  $Y$ . The correlation coefficient, which fluctuates between  $-1$  to  $+1$ , represents the linear association between two variables. It denotes the degree to which one variable changes with another. For positively correlated variables, their values increase or decrease together. When an alteration in one variable assumes a change in the other in the same direction, the Pearson correlation is strong and has a coefficient of  $+1$ . In the present work, the Pearson correlation coefficient was used to calculate the interrelation between different metals in each area. The Origin 2024b (learner version) software was utilized to analyze these correlations [52].

### 3.4. Factor analysis and cluster analysis:

Statistical methods are adopted for Factor and Cluster analysis using Origin Pro 2024b (learner version). Cluster analysis was performed on the original data utilizing Ward's method and Euclidean distance [36]. The factor-loading matrix was subjected to a varimax rotation to achieve a simple orthogonal structure. This rotation maximizes the variance of the squared loadings within each factor, resulting in a new matrix that facilitates interpretation. The explained variance for each variable was calculated based on the squared factor loadings. The residual variance for each variable was determined by summing the variances of the variable's factor loadings [37].

## 4. Result and discussions

### 4.1. Seasonal variations and spatial distribution of heavy metals.

In this study, pH ranged between 6.25 and 7.99, with the following seasonal variations: Monsoon (6.17–7.99), Pre-Monsoon (6.12–7.98), and Post-monsoon (6.42–7.62). These values indicate water quality varying from slightly acidic to slightly alkaline and within the permissible limit (6.5–8.5). Total Dissolved Solids (TDS), an indicator of groundwater salinity, ranged from 382 to 3652 ppm in this study.

Zinc (Zn) is vital for regulating human physiological and biological processes but can be harmful at elevated levels [38]. It is vital for protein synthesis. Zn levels in groundwater fluctuate primarily due to rock erosion and other natural phenomena [38; 39]. As per BIS IS 10500 (2012) [58], the acceptable range is 5000-15000  $\mu\text{g/L}$ . In this investigation, Zn concentrations in collected samples spanned from 0.89  $\mu\text{g/L}$  at KS-20 (Jabbalagudda) during Pre-monsoon to 112.2  $\mu\text{g/L}$  at KS-12 (Madinoor) during Monsoon, all within permissible limits. Figure 3.1 indicates increased Zn levels at KS-12 (Madinoor) across all seasons, potentially due to the study area's Granodioritic rocks, which are intermediate between granite and diorite and exhibit notable Zn concentrations. The variation in potassium-feldspar content in these rocks can influence overall mineral composition and, consequently, Zn levels.

The most prominent metallic element on Earth, aluminium (Al), makes up around 8% of the crust. It is found in nature as hydroxides, silicates, and oxides, in association with organic matter and elements such as fluoride and sodium. The amount of aluminum in aquatic environments varies substantially depending on mineralogical and physicochemical conditions. Drinking water with a pH of almost neutral usually has dissolved aluminium levels between 1 and 50  $\mu\text{g/L}$ , but in lower pH or organic-rich situations, these levels can rise to 500–1000  $\mu\text{g/L}$ . Dissolved aluminium abundances in very acidic fluids caused by the drainage of acid mines can be as high as 90000  $\mu\text{g/L}$  [40; 41]. In this study area, Al values in groundwater samples range from 8.72  $\mu\text{g/L}$  at KS-07 during Monsoon to 46.24  $\mu\text{g/L}$  at KS-02. According to BIS IS 10500 (2012), the acceptable limit is 30  $\mu\text{g/L}$  and the permissible limit is 200  $\mu\text{g/L}$ , with all values within the permissible range. Figure 3.2 shows that at KS-2 (Katarakigudlanoor), Al concentrations were high due to the presence of migmatite and granodioritic textures, which facilitate the leaching of Al into groundwater through mineral composition and weathering processes. At KS-11(Koppal) and KS-25 (Giniger), concentrations were moderately elevated throughout all seasons.

Arsenic(As), a highly toxic element, is naturally present in gemstones, water, and soil. Numerous groundwater samples exhibit elevated arsenic salt levels, resulting in contamination. The WHO recommends a maximum arsenic

concentration of 0.01 mg/L for safe water consumption. Increased arsenic exposure can cause symptoms such as diarrhea, diminished muscle strength, abdominal pain, skin itching, and vomiting. Prolonged exposure can lead to decreased blood cell production, skin discoloration, cardiac irregularities, nausea, and vascular rupture [42]. In this study, arsenic levels in groundwater samples range from -4.26 µg/L at KS-17 during the Post-monsoon period to 0.95 µg/L at KS-01 (Bisarahalli) during the Post-monsoon period, all within the permissible limit of 10-50 µg/L as per BIS IS 10500 (2012). According to the analysis from Figure 3.3 at KS-1 (Bisarahalli), high concentrations were recorded during the monsoon season, subsequently decreasing in the Pre-monsoon and Post-monsoon periods. Arsenic levels can significantly increase during the monsoon due to the influx of surface water and changes in groundwater dynamics. Following the monsoon, arsenic concentrations continue to decline as the groundwater system stabilizes, resulting in lower levels than during the monsoon period due to reduced water flow and less mobilization of arsenic from geological formations.

Cadmium(Cd) in groundwater mainly stems from corroded pipes, industrial effluents, and phosphate fertilizers. This toxic metal can cause vertigo, illness, digestive issues, seizures, and sensory impairments. High cadmium exposure may result in hepatic damage, bone fractures, malignancies, and cardiovascular and renal complications [43]. BIS IS 10500 (2012) stipulates a maximum allowable cadmium concentration of 3 µg/L. In this investigation, cadmium levels ranged from -0.48 µg/L at KS-21 (Basapur) to 0.47 µg/L at KS-15 (Sidaganahalli) during the Post-monsoon period, all within permissible limits. Figure 3.4 shows that cadmium concentrations increased during the monsoon and Post-monsoon seasons but decreased during the Pre-monsoon season at KS-11 (Koppal), KS-18 (Ganganal), and KS-19 (Kukanapalli). The rise in cadmium levels during the monsoon and Post-monsoon seasons in granodiorite and granite areas is primarily due to hydrological processes that enhance leaching and soil chemistry changes that increase cadmium solubility. Conversely, Dryer conditions that restrict leaching and movement are the cause of the decrease in cadmium levels during the pre-monsoon season.

Copper (Cu) is essential for human health, but excessive intake can damage the kidneys and liver, causing nausea, vomiting, and diarrhea [44]. Cu levels range from -0.5 µg/L at KS-10 (Halageri) during the monsoon season to 5.785 µg/L at KS-21 during the Post-monsoon season. The values recorded fall within the permissible limits (50 µg/L to 1500 µg/L as per BIS IS 10500: 2012), indicating the aquifer water is safe for drinking. According to spatial distribution maps of copper as shown in Fig. 3.5, concentrations increased at KS-12 (Madinoor) throughout all seasons but at KS-21 (Basapur), they increased during Post-monsoon and Pre-monsoon but decreased during the monsoon season. This observation can be attributed to various geological and hydrological factors.

Chromium (Cr) contamination in potable water supplies may originate by discharge from stainless steel, leather, printing materials, and dye industries; municipal refuse; oxidation of heating elements and bushings; or natural erosion of chromium mineral deposits [45]. Chromium concentrations range from 0.27 µg/L at KS-08 (Alawandi) during the monsoon season to 2.395 µg/L at KS-3 (Mattur) during the Post-monsoon season. BIS IS 10500 (2012) stipulates the chromium limit at 50 µg/L. The peak concentration of 2.395 µg/L indicates a substantial rise due to environmental changes, Post-monsoon. All observed values are within permissible limits for groundwater samples during these seasons. The spatial distribution of chromium is illustrated in Fig. 3.6.

The main sources of iron (Fe) in fresh water include minerals, silt, gravel, rusted metal, trash from mining, and industrial debris [46]. Fe concentrations range from 0.00 µg/L at KS-13 (Budshetnal) during the monsoon season to 180.94 µg/L at KS-12 (Madinoor) during the Post-monsoon season, as shown in Fig. 3.7. This variation indicates a significant rise in Fe levels Post-monsoon, likely due to changes in groundwater recharge and contamination processes.

In this study area, lead (Pb) concentrations in groundwater samples range from -1.30 µg/L at KS-08 (Alawandi) during the monsoon season to 3.11 µg/L at KS-24 (Karkihalli) during the Post-monsoon season. According to BIS IS 10500 (2012), the maximum allowable limit for Pb is 10 µg/L, and all observed values fall within this range. Overexposure to lead can cause kidney damage, hypertension, impulsiveness, cerebral impairment, hearing loss, cramping in the abdomen, and decreased fertility [47]. Figure 3.8 shows that Pb concentrations increase during the Post-monsoon and monsoon seasons due to leaching, rainfall patterns, sedimentation, and runoff accumulation, while they decrease during the Pre-monsoon season due to higher evaporation and reduced leaching at KS-22 (Huligi) and KS-24 (Karkihalli).

Manganese (Mn) is found in rocks, soils, surface, and groundwater. While trace amounts are necessary for human and animal health, excessive Mn can damage the nervous system, resulting in memory impairment and vision distortion. Elevated Mn levels can cause pulmonary embolism, respiratory infections, and Parkinson's syndrome [48]. BIS IS 10500 (2012) specifies the Mn limit for potable water as 100-300 µg/L, and all recorded values fall within this range. Mn concentrations vary from 0.002 µg/L at KS-6 (Belagatti) during the Pre-monsoon season to 164 µg/L at KS-21 (Basapur) during the monsoon season. The substantial increase in Mn levels during the monsoon season can be attributed to

factors such as runoff and sediment mobilization, which are prevalent during heavy rainfall periods. These seasonal variations are illustrated in Fig. 3.9.

Nickel (Ni) concentrations range from 0.01 µg/L at KS-20 (Jabbalagudda) during the monsoon season to 2.124 µg/L at KS-21 (Basapur) during the Post-monsoon season, indicating a significant rise Post-monsoon due to hydrological and mineral weathering changes. Nickel in water primarily results from mineral disintegration, wildfires, agricultural fertilizers, industrial effluents, and urban wastewater. Excessive nickel exposure in humans can cause liver, lung, kidney, bone, and brain damage, and potentially nasal cancer [49]. Figure 3.10 (GIS spatial distribution maps) shows elevated Ni concentrations at KS-11 (Koppal) and KS-8 (Alawandi) across all seasons, but a reduction at KS-17 (Hirebommanal) during the monsoon season. BIS IS 10500 (2012) sets the maximum allowable limit for Ni at 20 µg/L for drinking water, and all observed values are within this permissible limit.

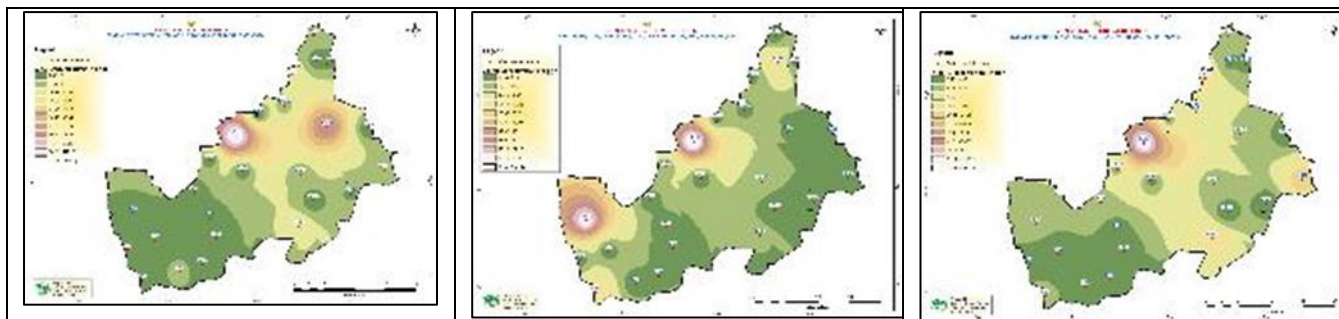


**Figure 3.1** Spatial Distribution of Zinc during Monsoon, Pre-monsoon and post-monsoon seasons

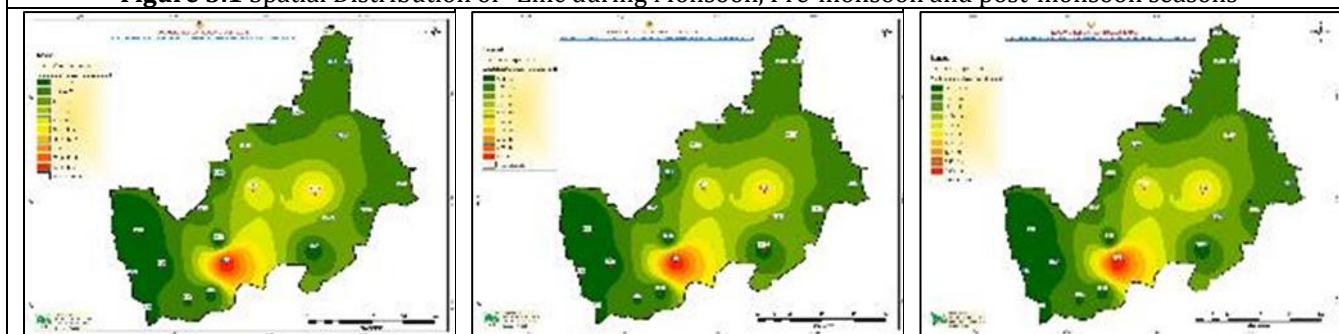


**Figure 3.2** Spatial Distribution of Aluminium during Monsoon, Pre-monsoon and post-monsoon seasons

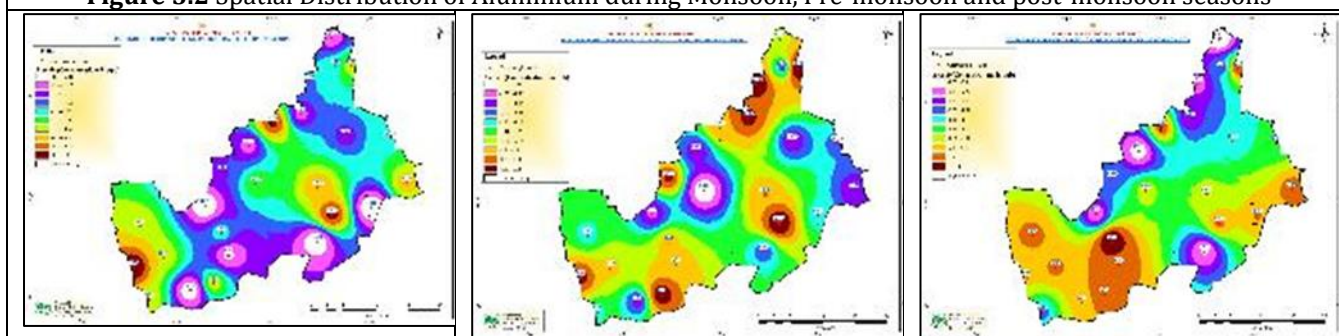


**Figure 3.3** Spatial Distribution of Arsenic during Monsoon, Pre-monsoon and Post-monsoon seasons



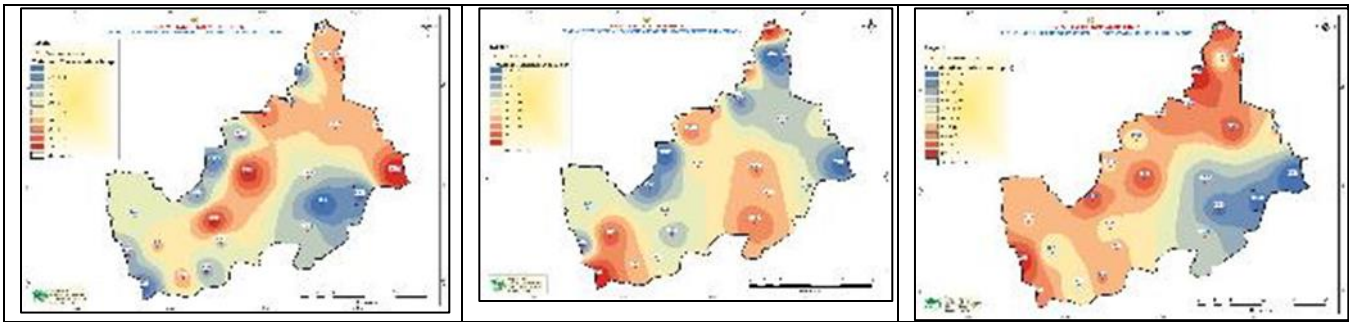


**Figure 3.4** Spatial Distribution of cadmium during Monsoon, Pre-monsoon and Post-monsoon seasons

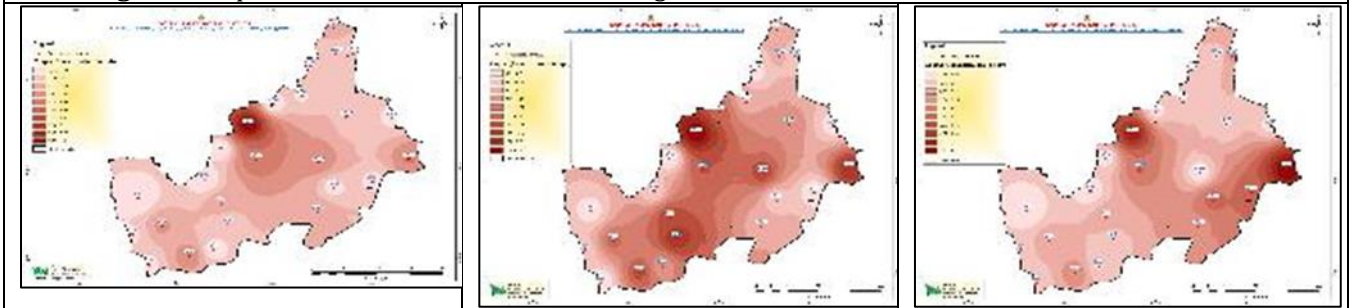


**Figure 3.5** Spatial Distribution of Copper during Monsoon, Pre-monsoon and Post-monsoon seasons

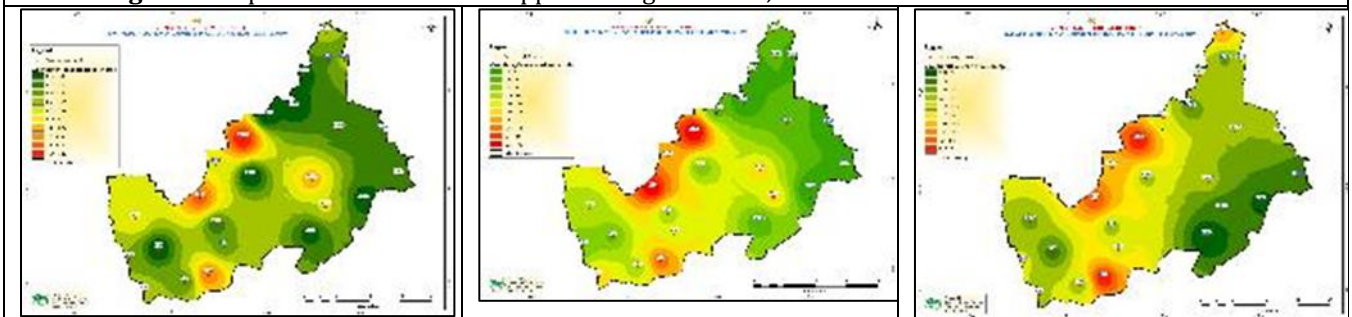


**Figure 3.6** Spatial Distribution of Chromium during Monsoon, Pre-monsoon and Post-monsoon seasons

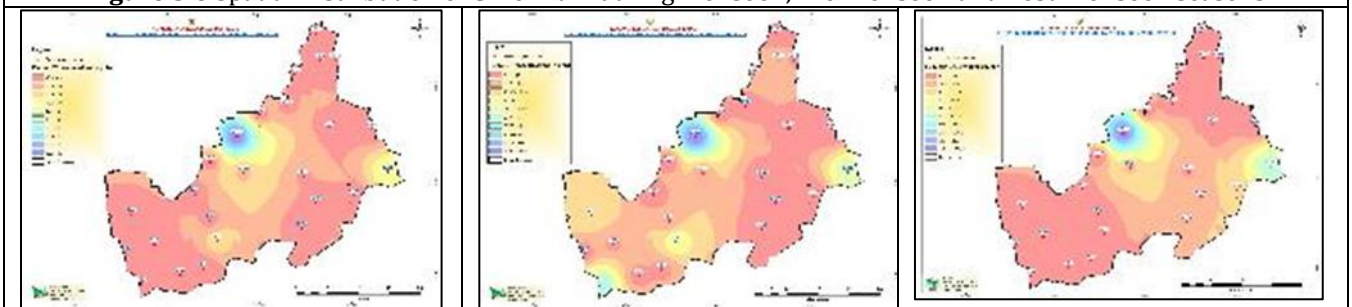


**Figure 3.7** Spatial Distribution of Ferrous during Monsoon, Pre-monsoon and Post-monsoon seasons

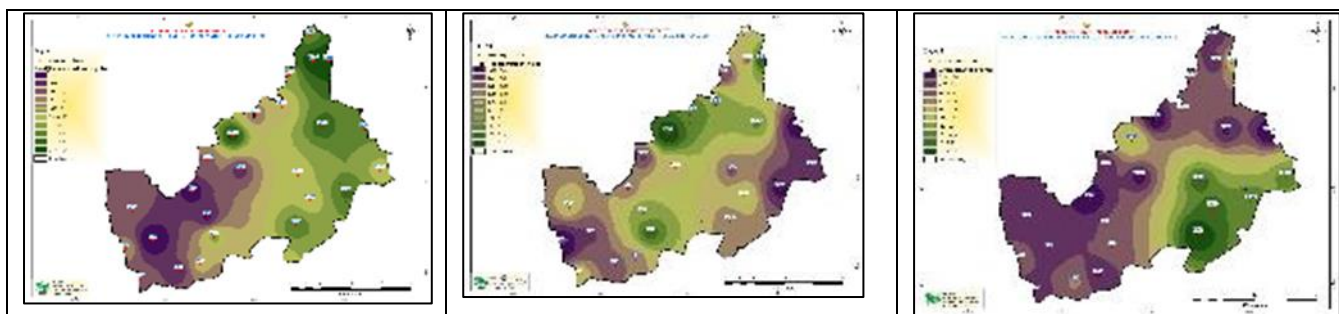


**Figure 3.8** Spatial Distribution of Lead during Monsoon, Pre-monsoon and Post-monsoon seasons

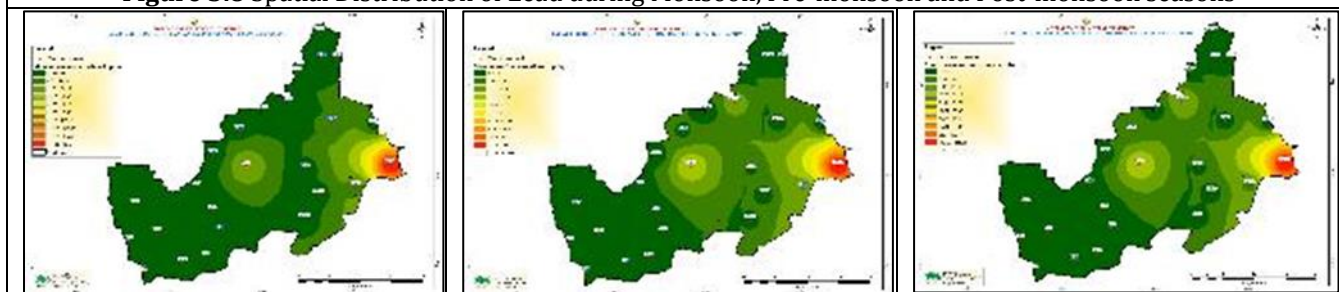


**Figure 3.9** Spatial Distribution of Manganese during Monsoon, Pre-monsoon and Post-monsoon seasons

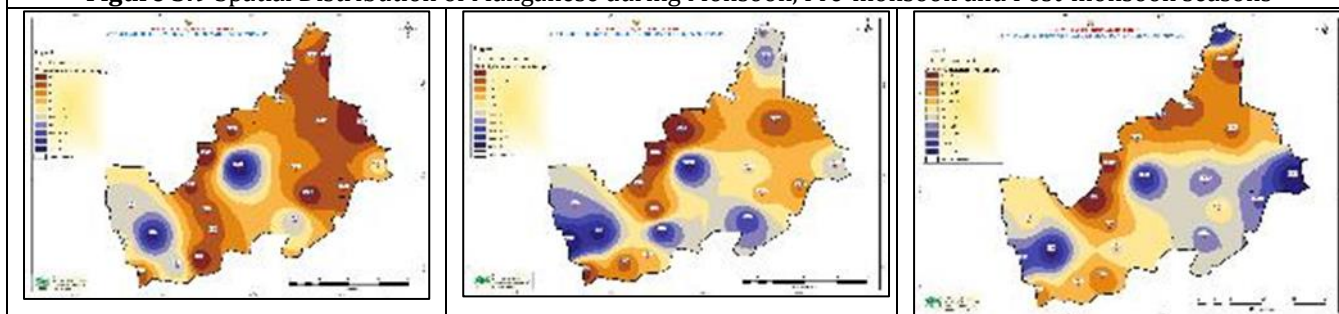


**Figure 3.10** Spatial Distribution of Nickel during Monsoon, Pre-monsoon and Post-monsoon seasons

**Figure 3** Variations in Spatial distribution of Heavy metals during Monsoon, Pre-monsoon, and Post-monsoon seasons

#### 4.2. Heavy metals pollution assessment

Pollution indices, including the HPI, MI, and  $I_{geo}$ , were computed using MS Excel 2010 to identify any heavy metal contamination in the study area's groundwater. Tables 03,04, and 05 also included descriptive analysis and results of calculated indices values conducted using Origin 2024b (learner version) software. The Heavy Metal Pollution Index assesses the completely current status of water by evaluating toxic and trace element proportions [50; 51]. When the HPI index result for any given groundwater sample is less than 100, it means that the sample is safe to drink. Within the context of this investigation, MI values span from -0.072 to 2.527, suggesting that samples KS-11(Koppal) and KS-12 (Madinoor) exhibit purity, whereas sample KS-21 (Basapur) demonstrates a slight degree of contamination across all seasons. In the current investigation,  $I_{geo}$  values for groundwater samples are predominantly negative; however, at KS-21 (Basapur), the  $I_{geo}$  value is slightly positive, indicating either uncontaminated or moderately contaminated (Table no .05).

**Table 3** Descriptive Statistics of heavy metals in groundwater during the Monsoon, Pre-monsoon, and Post-monsoon Seasons.

Heavy metal (in µg/L)	Pre-monsoon				Monsoon				Post-monsoon			
	Mean	S D	Min	Max	Mean	S D	Min	Max	Mean	S D	Min	Max
Al	2.124	1.153	0.90	5.72	0.90	10.46	-8.72	46.24	2.033	3.55	-3.64	11.412

As	-0.939	0.636	-2.39	0.047	-1.434	0.727	-2.52	0.013	-1.357	1.406	-4.26	0.95
Zn	10.34	19.13	0.89	74.88	11.069	24.75	0.93	112.2	10.67	21.47	1.14	109.37
Pb	-0.187	0.44	-1.02	0.854	-0.007	0.702	-1.30	1.34	0.475	1.108	-0.62	3.118
Cd	0.022	0.052	-0.07	0.142	0.236	0.064	0.11	0.364	0.073	0.242	-0.48	0.47
Ni	0.5584	0.278	0.1	1.151	0.416	0.428	0.01	1.726	0.969	0.521	0.142	2.124
Fe	10.634	16.83	1.49	77.69	0.013	0.061	-0.00	0.299	17.94	36.93	3.296	180.94
Cr	0.864	0.418	0.395	1.926	0.738	0.457	0.27	2.087	1.16	0.519	0.366	2.395
Cu	1.040	0.634	0.254	2.766	0.309	1.008	-0.50	4.478	2.511	1.052	1.484	5.785
Mn	5.697	20.14	0.002	100.2	8.212	33.05	-0.48	164.8	6.621	23.36	0.025	116.23

SD – Standard Deviation, Min – Minimum, Max – Maximum

**Table 4** Heavy metal pollution index (HPI) and Metal index (MI) value for Koppal Taluk groundwater samples during the Monsoon, Pre-monsoon, and post-monsoon seasons.

sampling station code	Sampling Station	Heavy metal pollution index(HPI)			Metal Index(MI)		
		Pre-monsoon	Monsoon	Post-monsoon	Pre-monsoon	Monsoon	Post-monsoon
KS-01	Bisarahalli	2.146	9.756	2.264	0.11	0.012	0.251
KS-02	Katarakigudlanoor	2.592	6.144	3.818	0.252	0.334	0.308
KS-03	Mattur	2.281	5.458	5.042	0.078	0.032	0.198
KS-04	Tigari	3.258	8.416	2.153	0.046	0.012	0.231
KS-05	Keslapur	4.459	5.207	5.65	0.25	-0.027	0.26
KS-06	Belagatti	3.979	3.979	9.88	0.004	0.055	0.371
KS-07	Kawaloor	2.064	7.142	3.462	0.111	0.043	0.193
KS-08	Alawandi	4.374	9.281	2.397	0.09	0.011	0.209
KS-09	Handral	2.724	6.973	6.777	0.008	-0.072	0.249
KS-10	Halageri	3.209	5.388	3.261	-0.019	-0.037	0.161
KS-11	Koppal	2.921	11.158	8.764	0.107	0.534	0.67
KS-12	Madinoor	4.607	7.547	6.044	0.518	0.324	1.116
KS-13	Budshetnal	2.842	7.963	5.887	0.119	0.052	0.142
KS-14	Irkalagada	2.166	6.895	7.268	0.071	0.04	0.39
KS-15	Sidaganahalli	3.371	5.383	11.09	0.051	0.077	0.325
KS-16	Chikkasulikeri	3.627	8.444	2.243	0.063	0.21	0.103
KS-17	Hirebommanal	3.426	7.275	7.069	0.084	0.129	0.289
KS-18	Ganganal	2.852	9.369	9.001	0.127	0.227	0.341
KS-19	Kukanapalli	1.794	8.205	7.431	0.061	0.256	0.21
KS-20	Jabbalagudda	3.322	7.09	4.562	-0.055	0.098	0.11
KS-21	Basapur	6.948	14.8379	19.75	1.372	2.525	2.277
KS-22	Huligi	3.037	5.807	13.543	-0.031	0.173	0.48

KS-23	Hirekasanakan di	2.317	3.604	13.382	0.126	0.064	0.333
KS-24	Karkihalli	3.562	6.891	9.902	0.066	0.11	0.47
KS-25	Ginigera	3.238	5.957	10.666	0.084	0.206	0.364

**Table 5** Geo accumulation index ( $I_{geo}$ ) value for Koppal Taluk groundwater samples during the Monsoon, Pre-monsoon, and Post-monsoon seasons.

Sampling Station Code	Al	As	Zn	Pb	Cd	Ni	Fe	Cr	Cu	Mn
KS-01	-7.81	-3.817	-13.16	-8.7	-6.44	-5.33	-6.3	-6.19	-4.9	-9.16
KS-02	-10.2	-4.108	-13.96	-6.37	-5.42	-4.783	-5.526	-5.93	-5.15	-6.68
KS-03	-8.29	-5.027	-13.27	-5.79	-4.82	-5.555	-6.91	-4.97	-5.29	-12
KS-04	-11.6	-4.743	-13.72	-5.29	-11.1	-5.262	-6.613	-6.18	-4.72	-8.3
KS-05	-8.93	-4.463	-11.73	-6.62	-4.44	-5.52	-5.277	-6.08	-5.25	-7.61
KS-06	-7.31	-4.303	-12.77	-6.21	-3.48	-4.387	-7.023	-6.01	-5.16	-10.2
KS-07	-6.36	-4.158	-11.74	-6.1	-5.66	-4.884	-6.436	-6.31	-5.66	-9.54
KS-08	-8.14	-5.341	-14.26	-6.13	-12.1	-3.967	-5.653	-6.77	-4.89	-7.47
KS-09	-8.14	-5.341	-14.26	-6.13	-12.1	-3.967	-5.653	-6.77	-4.89	-7.47
KS-10	-7.86	-5.303	-11.53	-6.51	-5.73	-6.214	-6.727	-5.5	-5.41	-10.6
KS-11	-6.83	-5.027	-12.84	-5.38	-4.04	-4.1	-4.592	-6.14	-4.55	-2.23
KS-12	-5.33	-4.693	-7.684	-3.31	-6.11	-5.267	-1.314	-4.97	-3.85	-4.99
KS-13	-7.13	-5.743	-11.71	-4.67	-4.67	-5.764	-6.584	-6.06	-5.4	-10.3
KS-14	-8.28	-5.966	-11.07	-6.31	-4.51	-5.804	-6.572	-6.41	-5.19	-3.1
KS-15	-7.08	-6.397	-10.24	-6.46	-3.25	-5.436	-6.292	-6.07	-5.21	-8.74
KS-16	-9.07	-9.288	-12.5	-5.99	-8.05	-5.904	-6.047	-6.34	-5.3	-7.11
KS-17	-6.97	-6.397	-11.75	-6.26	-4.24	-4.085	-5.952	-5.47	-4.9	-9.34
KS-18	-7.32	-6.288	-12.71	-3.97	-3.9	-6.265	-6.216	-6.05	-4.83	-10
KS-19	-6.64	-6.091	-11.37	-5.7	-4.01	-5.637	-6.785	-6.21	-5.28	-8.3
KS-20	-8	-6.118	-13.14	-4.59	-5.52	-5.103	-7.093	-6.19	-5.37	-10.6
KS-21	-4.94	-5.381	-9.821	-2.86	-3.21	-3.82	-2.582	-6.84	-3.7	0.147
KS-22	-4.72	-5.506	-14.24	-2.77	-3.51	-4.475	-4.05	-7.08	-4.45	-4.55
KS-23	-5.61	-5.693	-13.89	-2.67	-3.54	-5.026	-5.247	-6.84	-4.49	-10.7
KS-24	-9.72	-9.288	-10.11	-2.27	-5.12	-4.591	-4.59	-7.68	-4.77	-7.37
KS-25	-6.11	-7.446	-11.78	-2.65	-4.26	-4.495	-5.374	-6.17	-5.54	-6.51

#### 4.3. Pearson correlation

The groundwater quality parameters' correlation matrix, in terms of sample correlation coefficient ( $r$ ) and significant level ( $\rho$ ) presented in Tables 6, 7, and 8, showed that samples with ( $r > 0.75$ ) were strongly correlated at a significance level ( $\rho < 0.05$ ), while those with ( $0.5 < r < 0.75$ ) indicated a moderate association at the same significance level. The analysis demonstrated that some parameters have a strong association, suggesting a common source or similar trend due to factors like water-rock interaction and ion exchange. Additionally, samples with ( $0.01 < r < 0.5$ ) showed a feeble,

and a perfect adverse association was observed when ( $r < 0$ ) at a significance level ( $\rho < 0.05$ ) [52]. Heavy metals in this study exhibit generally minor association with the other parameters, indicating their source of origin may be affected by more independent processes. However, various factors affect the intensity of heavy metals in water, like geological setting of the water bearing zones, hydrogeological conditions, status of soil, industrial release, water acidity, water oxidation characteristics, and so on [53].

In the Post-monsoon period, zinc exhibits a robust positive correlation with nickel and cadmium, whereas Ni shows a notable interrelation with Cd, suggesting that analogous anthropogenic activities or geological formations may impact both elements. Pb demonstrates a moderate association with Cu, Zn, and Cd. The co-occurrence of Pb with these metals can escalate concerns about cumulative toxicity and environmental health risks. Manganese displays an inverse relationship with zinc, arsenic, iron, and chromium throughout the year.

During the monsoon season, Fe exhibits a significant correlation with Zn and Cd, likely due to increased heavy metal mobility, biogeochemical cycling, and soil properties. Pb shows a moderate association with Zn and Fe. The co-occurrence of Pb with Zn and Fe in environmental samples raises concerns about potential health risks, as these metals can bioaccumulate and pose toxicity threats to aquatic organisms and humans. There is a substantial positive association between (Pb and Al), (Cd and Zn), and (Fe and Ni) during the pre-monsoon season. Arsenic negatively correlates with Zn, Ni, and Cu across all seasons. These correlations underscore the complex interactions among heavy metals in aquatic environments, especially during the Pre-monsoon season when runoff and sedimentation are pronounced. Understanding these relationships is essential for assessing ecological risks and formulating pollution management strategies.

**Table 6** The correlation matrix of heavy metals in groundwater during Post-monsoon season for Koppal Taluk

	Al	As	Zn	Pb	Cd	Ni	Fe	Cr	Cu	Mn
Al	1.000*									
As	-0.111*	1.000*								
Zn	0.376*	-0.468*	1.000*							
Pb	0.588*	-0.018*	0.288*	1.000*						
Cd	-0.591*	-0.276*	-0.043*	-0.722*	1.000*					
Ni	0.243*	0.131*	-0.023*	0.321*	-0.390*	1.000*				
Fe	0.540*	-0.286*	<b>0.946*</b>	0.380*	-0.258*	0.162*	1.000*			
Cr	-0.073*	-0.310*	0.414*	-0.378*	0.425*	-0.377*	0.325*	1.000*		
Cu	<b>0.690*</b>	-0.011*	<b>0.603*</b>	<b>0.546*</b>	-0.520*	0.471*	<b>0.786*</b>	-0.059*	1.000*	
Mn	0.480*	0.153*	0.144*	0.281*	-0.451*	0.505*	0.339*	-0.218*	0.679*	1.000*

2tailed test of significance is used; \* Correlation is significant at a 0.05 level

**Table 7** The correlation matrix of heavy metals in groundwater during the Pre-monsoon season for Koppal Taluk.

	Al	As	Zn	Pb	Cd	Ni	Fe	Cr	Cu	Mn
Al	1.000*									
As	-0.064*	1.000*								
Zn	-0.193*	-0.245*	1.000*							
Pb	0.275*	0.051*	0.402*	1.000*						
Cd	0.038*	-0.049*	0.111*	0.102*	1.000*					
Ni	0.204*	0.024*	-0.227*	-0.285*	-0.071*	1.000*				
Fe	0.115*	-0.266*	0.728*	0.472*	0.222*	-0.284*	1.000*			
Cr	0.188*	-0.099*	0.405*	0.302*	0.054*	-0.425*	0.474*	1.000*		

<b>Cu</b>	0.458*	-0.298*	0.227*	0.464*	0.087*	0.056*	0.514*	0.259*	1.000*	
<b>Mn</b>	0.120*	-0.302*	-0.080*	-0.196*	-0.277*	0.143*	0.204*	-0.194*	0.305*	1.000*

2tailed test of significance is used; \* Correlation is significant at a 0.05 level

**Table 8** The correlation matrix of heavy metals in groundwater during the Monsoon season for Koppal Taluk.

	<b>Al</b>	<b>As</b>	<b>Zn</b>	<b>Pb</b>	<b>Cd</b>	<b>Ni</b>	<b>Fe</b>	<b>Cr</b>	<b>Cu</b>	<b>Mn</b>
<b>Al</b>	1.000*									
<b>As</b>	-0.170*	1.000*								
<b>Zn</b>	0.003*	-0.243*	1.000*							
<b>Pb</b>	0.188*	-0.145*	0.413*	1.000*						
<b>Cd</b>	-0.030*	0.107*	-0.054*	-0.082*	1.000*					
<b>Ni</b>	-0.041*	0.078*	-0.140*	-0.459*	0.418*	1.000*				
<b>Fe</b>	0.143*	-0.142*	0.817*	0.318*	0.004*	-0.071*	1.000*			
<b>Cr</b>	0.028*	-0.068*	0.457*	0.105*	-0.386*	-0.406*	0.559*	1.000*		
<b>Cu</b>	0.090*	-0.159*	0.754*	0.214*	0.200*	0.223*	0.890*	0.393*	1.000*	
<b>Mn</b>	-0.025*	0.154*	-0.012*	0.036*	0.462*	0.167*	0.199*	-0.127*	0.180*	1.000*

2tailed test of significance is used; \* Correlation is significant at a 0.05 level

#### 4.4. Factor analysis

factor analysis with Varimax Rotation (Kaiser Normalisation) in Origin Pro 2024b (learner version) software was used to identify the contamination factors. The sorted Varimax rotated factor loadings of the principle components obtained by PCA, together with the eigenvalues, cumulative per cent, and percentage variance, are shown in Table 9. The analysis of 10 water quality indicators yielded 10 components, but based on eigenvalues ( $\geq 1$ ), only the first three factors were deemed significant, explaining the variance in hydrogeological data. Anthropogenic inputs and weathering processes are the main factors influencing the geochemical makeup of groundwater (35).

The first three principal components (PCs) in this analysis were found to be 62.10%, 65.10%, and 77.17% of the cumulative variance, respectively, for the pre-monsoon, monsoon, and post-monsoon seasons. PC1 accounted for 30.39%, PC2 for 18.16%, and PC3 for 13.55% of the disparity in the Pre-monsoon sample. PC1 explained 32.43%, PC2 20.72%, and PC3 11.96% of the degree of variability in the monsoon season dataset. During the Post-monsoon season, PC1 explained 42.14%, PC2 accounted for 25.12%, and PC3 explained 9.91% of the variance (Table 9). Factor loadings are divided into three categories by Narsimha et al. (2018) [54]: strong, moderate, and weak. These categories correspond to unconditional load values of  $>0.75$ ,  $0.75-0.50$ , and  $0.50-0.30$ , respectively.

Factor 1 exhibits a robust positive loading of Zn and Fe across all seasons, indicating that human activities such as agriculture, urban runoff, and geogenic processes influence the seasonal distribution of these metals. Significant contributors include evaporation and the dissolution of rock formations.

Factor 2 displays a strong positive loading of Cd during the monsoon, Pb occurs during the Post-monsoon season, while Cu and Al occur during the pre-monsoon season. The presence of cadmium in the monsoon may be attributed to agricultural runoff and leaching from contaminated soils, while Cu and Al in the Pre-monsoon may result from urban runoff, industrial discharges, and soil erosion. Pb in the Post-monsoon season likely stems from residual contamination from the Monsoon and urban sources.

In the Pre-monsoon and Post-monsoon seasons, Factor 3 shows a strong positive connection with Mn, but in all seasons, it shows negative loadings between Cd and Cr. Mechanisms of nature including mineral weathering, oxide and hydroxide breakdown, and geological formations are probably the cause of elevated Mn concentrations. The adverse relationship between Cd and Cr suggests an inverse correlation with other factors affecting groundwater quality, such as pH, oxidation-reduction potential (ORP), and seasonal dilution.

**Table 9** Rotated component matrix of Three-factor model.

	Monsoon			Pre-monsoon			Post-monsoon		
Variable	Rotated Loadings by Varimax Method								
	Factor 1	Factor 2	Factor 3	Factor 1	Factor 2	Factor 3	Factor 1	Factor 2	Factor 3
Al	-0.050	0.097	0.676	-0.154	0.876	-0.036	0.400	0.653	0.317
As	-0.122	0.095	-0.484	-0.262	-0.054	-0.673	-0.607	0.014	0.373
Zn	0.875	-0.066	0.213	0.833	-0.061	0.161	0.939	0.131	0.089
Pb	0.248	-0.124	0.734	0.547	0.520	-0.281	0.148	0.915	0.106
Cd	-0.012	0.848	-0.017	0.242	0.135	-0.315	0.088	-0.824	-0.348
Ni	-0.030	0.679	-0.404	-0.617	0.257	0.207	-0.136	0.224	0.733
Fe	0.947	0.068	0.178	0.809	0.294	0.279	0.873	0.240	0.328
Cr	0.654	-0.537	-0.060	0.666	0.203	-0.163	0.625	-0.533	-0.182
Cu	0.906	0.288	0.073	0.304	0.762	0.329	0.520	0.436	0.676
Mn	0.132	0.654	0.038	-0.152	0.148	0.836	0.091	0.199	0.855
Eigen Value	3.243	2.072	1.196	3.039	1.816	1.355	4.214	2.512	0.991
% of total Variance	32.428	20.716	11.965	30.389	18.163	13.553	42.143	25.118	9.913
% of cumulative variance	32.428	53.143	65.108	30.389	48.553	62.105	42.143	67.261	77.174

Extraction method: Principal component analysis. Rotation method: Varimax with Kaiser Normalization. Rotation converged in 5 iterations, % - Percentage.

#### 4.5. Cluster analysis

Exploration HCA was carried out on the heavy metals for the present study to divide the heavy metal sources into anthropogenic and natural groups. Figure 4.1, 4.2 and 4.3 demonstrate the Hierarchical dendrogram of the results. A lower distance cluster value represents a dependence of higher significance [55]. During all the seasons, Zn and Fe have lower distances representing these might be the most significant contamination factors, which is the same as predicted in factor analysis. Zn is introduced into groundwater may be due to human-induced pollution and Fe due to natural sources like rock-water interaction.

In cluster1, during the Pre-monsoon and Post-monsoon seasons, Al, Fe, Cu, Zn and Pb have the same sources for their origin in the present study as shown in Fig. 4.2 and 4.3. Cluster 2 contains arsenic only, which indicates that it originated from municipal waste and industrial waste like paint, leather and pesticides [56]. Saha and Rahman [57] proposed three principal sources of surface water metal contamination: a) industrial effluents (Pb, Ni, Cu, Zn, and As), b) municipal wastes (Cr, Cu, and Mn), and c) atmospheric deposition (Cd). The present study suggests that arsenic and Cr may be released from paint and leather industries, while Cd, Zn, Cu, and Pb may have originated from industrial and atmospheric deposition, and Ni and Mn may have dissolved from agricultural and industrial sources.

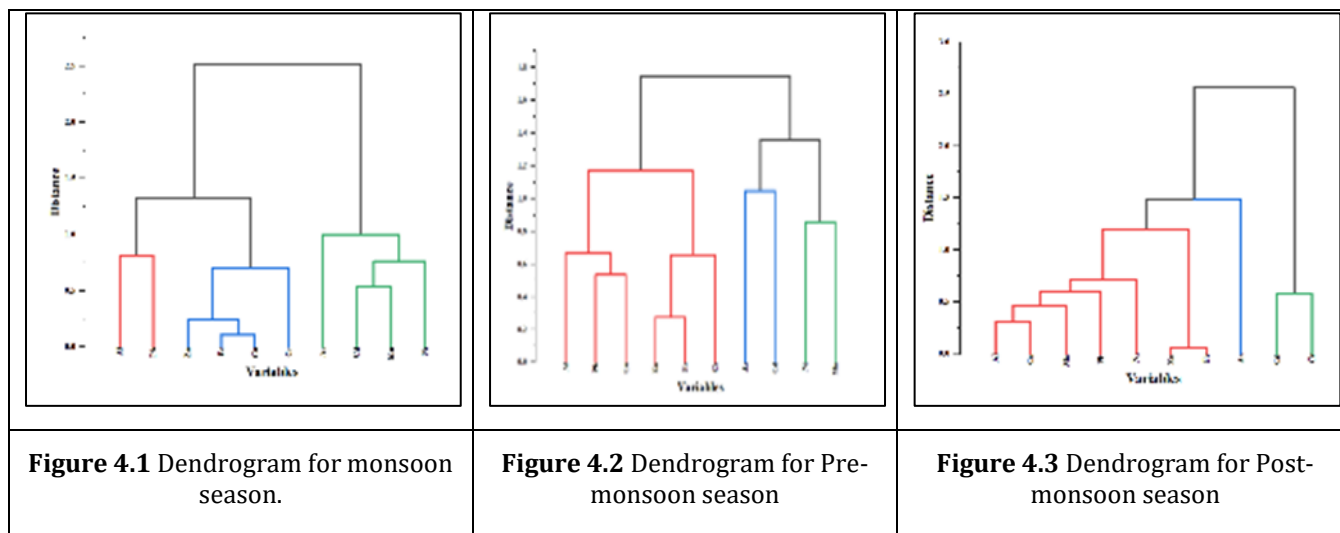


**Figure 4** Dendrogram diagram for Variables during Monsoon, Pre-monsoon and Post-monsoon seasons.

## 5. Conclusion

Groundwater specimens were gathered from December 2022 to November 2023. The methodology for identifying and measuring the sources, levels of contamination, and spatial distribution of heavy metals in groundwater in and around Koppal Taluk is presented in this study. The assessment of heavy metals was conducted utilizing ICP-OES spectroscopy, with findings remaining within the acceptable parameters established by BIS IS 10500: 2012 and WHO guidelines. Heavy metal contamination was assessed using HPI, MI, and  $I_{geo}$  indices in and around Koppal taluk. Most  $I_{geo}$  values were less than 1, indicating uncontaminated to moderately contaminated water. HPI values were below 100, showing safe drinking water. From the obtained MI data figures, it varied between 0 and 2, with the majority of samples demonstrating an absence of metal contamination. Metals in groundwater samples are ranked by mean concentration in a decreasing manner as follows: Fe > Zn > Mn > Al > Cu > Cr > Ni > Cd > Pb > As. The findings show that concentrations of heavy metals in the collected samples are below WHO guideline levels, implying that the groundwater samples are free from metal contamination and safe for consumption. The main cause of water contamination, as shown by multivariate statistical modelling, is human endeavours, and urban and agricultural runoff.

Factor analysis and cluster analysis representing Zn, Fe and Cu having less cluster distance, which might significantly contribute to groundwater pollution. Zn and Cu from human-induced pollution and Fe from natural sources.

The tool ArcGIS 10.8 used in this study was highly effective for data aggregation, transmission, visualization, and spatial data overlay. The IDW (Inverse Distance Weighting) interpolation method significantly aids in determining heavy metal distribution without extensive field or lab research. The unique analysis highlights the critical role of GIS in assessing groundwater quality and equips decision-makers with essential information for implementing effective monitoring strategies to manage groundwater resources in the region. Integrating innovative approaches combining statistical, geographical methods, and indices provides a holistic methodology for effectively assessing water quality. Policymakers can adopt a similar methodology to identify and monitor critical variables that need to be managed to improve water quality effectively.

## Compliance with ethical standards

### Acknowledgments

I am very thankful to “Veerashaiva Vidyavardhaka Sangha Ballari (R)” for carrying out my further studies and research activities. Also thankful to Mr. Guruswamy, the project Manager of NRDMS centre, Zilla Panchayath Koppal for providing the ArcGIS tool to understand the spatial distribution of heavy metals in Koppal groundwater.

### Disclosure of conflict of interest

The authors declare that they have no known competing financial interests or personal relationships that would influence this paper.



### Funding Sources

The author(s) received no financial support for the research, authorship, and/or publication of this article.

---

### References

- [1] Khan R, Dalchand J. Groundwater quality assessment for drinking purposes in Raipur City, Chhattisgarh using water quality index and geographic information system. *J Geol. Soc. India.* 2017; 90:69–76. <https://doi.org/10.1007/s12594-017-0665-0>
- [2] Sudarshana Reddy Y, Sunitha V, Suvarna B. Monitoring of groundwater quality for drinking purposes using the WQI method and its health implications around inactive mines in Vemula-Vempalli region, Kadapa District, South India. *Springer Applied Water Science.* 2020a; 10(8):202. <http://dx.doi.org/10.1007/s13201-020-01284-2>
- [3] Sudarshana Reddy Y, Sunitha V, Suvarna, B. Groundwater quality evaluation using GIS and water quality index in and around inactive mines, Southwestern parts of Cuddapah basin, Andhra Pradesh, South India. *Springer Hydro Research.* 2020b; 3:146-157. <http://dx.doi.org/10.1016/j.hydres.2020.11.001>
- [4] osar Hikmat Hama Aziz, Fryad S Mustafa, Khalid M Omer, Sarkawt Hama, Rebaz Fayaq Hamarawf and Kaiwan Othman Rahman. Heavy metal pollution in the aquatic environment: efficient and low-cost removal approaches to eliminate their toxicity: a review *RSC Adv.* 2023; 13:17595-17610. <https://doi.org/10.1039/D3RA00723E>
- [5] USEPA (1998) National recommended water quality criteria. *Fed Reg* 63(234):67548–67558.
- [6] Virág L, Erdodi F, Gergely P. *Bioinorganic chemistry for medical students.* Scriptum University of Debrecen, Hungary. 2016; 1–104.
- [7] Xiao J, Wang L, Deng L, Jin Z. Characteristics sources water quality and health risk assessment of trace elements in river water and well water in the Chinese Loess Plateau. *Sci Total Environ.* 2019; 650:2004–2012.
- [8] Ahamad A, Raju NJ, Madhav S, Khan AH. Trace elements contamination in groundwater and associated human health risk in the industrial region of southern Sonbhadra, Uttar Pradesh, India. *Environ Geochem Health.* 2020; 42:3373–3391.
- [9] Tong S, Li H, Tudi M, Yuan X, Yang L. Comparison of characteristics water quality and health risk assessment of trace elements in surface water and groundwater in China. *Ecotoxicol Environ Safety* 2021; 219:112283.
- [10] Yousefi M, Ghoochani M, Mahvi AH. Health risk assessment to fluoride in drinking water of rural residents living in the Poldasht city, Northwest of Iran. *Ecotoxicol Environ Saf.* 2018; 148:426–430.
- [11] WHO Guidelines for drinking-water quality: incorporating the first and second addenda. World Health Organization, Switzerland. 2022.
- [12] Arslan H, Ayyildiz Turan, N. Estimation of Spatial Distribution of Heavy Metals in Groundwater Using Interpolation Methods and Multivariate Statistical Techniques; Its Suitability for Drinking and Irrigation Purposes in the Middle Black Sea Region of Turkey. *Environ. Monit. Assess.* 2015; 187:516.
- [13] S, Shahid M, Natasha, Shah AH, Saeed F, Ali M, Qaisrani, SA, Dumyat C. Heavy Metal Contamination and Exposure Risk Assessment via Drinking Groundwater in Vehari, Pakistan. *Environ. Sci. Pollut. Res.* 2020; 27:39852–39864.
- [14] Long X, Liu F, Zhou X, Pi J, Yin W, Li F, Huang S. Estimation of Spatial Distribution and Health Risk by Arsenic and Heavy Metals in Shallow Groundwater around Dongting Lake Plain Using GIS Mapping. *Chemosphere* 2021; 269:128698.
- [15] Mishra S, Amit Kumar, Silpa Yadav, Singhal MK. Assessment of heavy metal contamination in water of Kali River using principle component and cluster analysis, India. *Sustain. Water Resour. Manag.* 2018; 4: 573–581. <https://doi.org/10.1007/s40899-017-0141-4>
- [16] [16] Nasrabadi, T. An index approach to metallic pollution in river waters. *Int. J. Environ. Res.* 2015; 9(1): 385–394.
- [17] Kannel PR, Lee S, Kanel SR, Khan SP, Lee YS. Spatial–temporal variation and comparative assessment of water qualities of urban river system: a case study of the river Bagmati (Nepal). *Environmental Monitoring and Assessment.* 2007; 129:433–459.

- [18] Arora S, Keshari AK. Pattern recognition of water quality variance in Yamuna River (India) using hierarchical agglomerative cluster and principal component analyses. *Environmental Monitoring and Assessment*. 2021; 193(8):494.
- [19] Loska K, Wiechuła, D. Application of principal component analysis for the estimation of source of heavy metal contamination in surface sediments from the Rybnik reservoir. *Chemosphere*. 2003; 51(8):723-733.
- [20] Filgueiras AV, Lavilla I, Bendicho C. Evaluation of distribution, mobility and binding behaviour of heavy metals in surficial sediments of Louro river (Galicia, Spain) using chemometric analysis: a case study. *Science of the Total Environmen*. 2004; 330(1-3):115-129.
- [21] Ting YS, Freeman KC, Kobayashi C, De Silva GM, Bland-Hawthorn J. Principal component analysis on chemical abundances spaces. *Monthly Notices of the Royal Astronomical Society*. 2012; 421(2):1231-1255.
- [22] Zhao G, Ye S, Yuan H, Ding X, Wang J. Surface sediment properties and heavy metal pollution assessment in the Pearl River Estuary, China. *Environmental Science and Pollution Research*. 2017;24(3):2966-2979.
- [23] Central Ground Water Information Booklet (CGWIB-1954), Koppal District, Karnataka, Govt of India Ministry of Water Resources Central Ground Water Board republished on Feb 2013.
- [24] APHA Standard Methods for the Analysis of Water and Wastewater. 15th Edition, American Public Health Association and Water Pollution Control Federation, Washington DC. 2000;12-56.
- [25] iCAP PRO Series ICP-OES operating manual BRE0016949 Revision c Thermo Fisher Scientific (Bremen) GmbH, Hanna-Kunath-Str. 11, 28199 Bremen, Germany 2020.
- [26] Prasad B, Sangita K. Heavy Metal Pollution Index of Ground Water of an Abandoned Open Cast Mine Filled with Fly Ash: A Case Study. *Mine Water Environ*. 2008; 27:265-267. <https://doi.org/10.1007/s10230-008-0050-8>
- [27] Reza R, Singh G. Heavy metal contamination and its indexing approach for river water. *Int. J. Environ. Sci. Technol*. 2010; 7:785-792. <https://doi.org/10.1007/BF03326187>
- [28] Bhuiyan MAH, Suruvi NI, Dampare SB, Islam MA, Shamshad BQ, Samuel Ganyaglo, Shigeyuki Suzuki. Investigation of the possible sources of heavy metal contamination in lagoon and canal water in the tannery industrial area in Dhaka, Bangladesh. *Environ Monit Assess*. 2011; 175:633-649. <https://doi.org/10.1007/s10661-010-1557-6>
- [29] Tamasi G, Cini R. Heavy Metals in Drinking Waters from Mount Amiata (Tuscany, Italy) Possible Risks from Arsenic for Public Health in the Province of Siena. *Sci Total Environ*. 2004;327(1-3):41-51. <http://dx.doi.org/10.1016/j.scitotenv.2003.10.011>
- [30] Muller G. Index of geo-accumulation in sediments of Rhine River. *Geochemical Journal*. 1969; 2:108-118. <https://api.semanticscholar.org/CorpusID:128079163>
- [31] Radi, NFA, Zakaria R, Azman MA. Estimation of missing rainfall data using spatial interpolation and imputation methods. In AIP conference proceedings. American Institute of Physics. 2015; 1643:42. <https://doi.org/10.1063/1.4907423>
- [32] Bhunia GS, Keshavarzi A, Shit PK, et al. Evaluation of groundwater quality and its suitability for drinking and irrigation using GIS and geostatistics techniques in semiarid region of Neyshabur, Iran. *Appl Water Sci*. 2018; 8:168. <https://doi.org/10.1007/s13201-018-0795-6>
- [33] Jinan Abdul Ameer Abbas. Spatial distribution of some of heavy metals pollution parameters for soils surrounding al- dora power plant, South Baghdad. *Iraq Plant Archives*. 2020; 20(2):6639-6654.
- [34] Unnati Chaudhary, Asit Singh, Saumya Singh. Analysis of groundwater parameters in Lucknow, Uttar Pradesh using GIS-based & change detection maps. *World Journal of Advanced Research and Reviews*. 2023; 19(03):1237-1246. <https://doi.org/10.30574/wjarr.2023.19.3.1964>
- [35] Chan RY. Determinants of Chinese Consumers' Green Purchase Behavior. *Psychology & Marketing*. 2001; 18:389-413. <https://doi.org/10.1002/mar.1013>
- [36] Marghade D, Malpe DB, Subba Rao N. Applications of geochemical and multivariate statistical approaches for the evaluation of groundwater quality and human health risks in a semi-arid region of eastern Maharashtra, India. *Environ. Geochem. Health*. 2021; 43:683-703. <https://doi.org/10.1007/s10653-019- 00478-1>
- [37] Ratnakar Dhakate. Characterization of groundwater salinity by hydrogeochemical and multivariate statistical analysis in the coastal aquifer of Nagapattinam district, Southern India. *Heliyon*. 2024 ;10(11): e32396. <https://doi.org/10.1016/j.heliyon.2024.e32396>

- [38] Kumar AR, Riyazuddin P. Speciation of selenium in groundwater: seasonal variations and redox transformations. *J. Hazard. Mater.* 2011; 192(1):263–269. <https://doi.org/10.1016/j.jhazmat.2011.05.013>
- [39] Rajappa B, Puttaiah ET, Manjappa S. Monitoring of heavy metal concentration in groundwater of Hakinaka Taluk, India. *Contemp. Eng. Sci.* 2010; 3(4):183–190.
- [40] Hicks JS, Hackett DS, Sprague G L. Toxicity and aluminium concentration in bone following dietary administration of two sodium aluminium phosphate formulations in rats. *Food Chem Toxicol.* 1987; 25(7):533–538. [https://doi.org/10.1016/0278-6915\(87\)90205-5](https://doi.org/10.1016/0278-6915(87)90205-5)
- [41] Momot O, Synzynys B. Toxic aluminium and heavy metals in groundwater of middle Russia: health risk assessment. *Int J Environ Res Public Health.* 2005;2(2):214–218. <https://doi.org/10.3390%2Fijerph2005020003>
- [42] Wadhwa SK, Kazi TG, Chandio AA, Afridi HI, Kolachi NF, Khan S, Kandhro GA, Nasreen S, Shah AQ, Baig JA. Comparative study of liver cancer patients in arsenic exposed and non-exposed areas of Pakistan. *Biological Trace Element Research.* 2011;144(1–3):86–96. <http://dx.doi.org/10.1007/s12011-011-9036-7>
- [43] cLaughlin MJ, Parker DR, Clarke JM. Metals and micronutrients– Food safety issues. *Field Crops Research.* 1999; 60(1–2):143–163. [https://doi.org/10.1016/S0378-4290\(98\)00137-3](https://doi.org/10.1016/S0378-4290(98)00137-3)
- [44] Pawlisz AV, Kent RA, Schneider UA, Jefferson C. Canadian water quality guidelines for chromium. *Environmental Toxicology and Water Quality.* 1997; 12(2):123-183. <https://www.webofscience.com/wos/WOSCC/full-record/A1997WV37300004>
- [45] Dixit S, Tiwari S. Impact assessment of heavy metal pollution of Shahpura Lake, Bhopal, India. *Int. J. Environ. Res.* 2008; 2(1):37–42.
- [46] Supantha P, Umesh M. Assessment of underground water quality in North Eastern region of India: A case study of Agartala City. *International Journal of Environmental Sciences.* 2011; 2(2):850–862.
- [47] Mohan BS, Hosetti BB. Aquatic plants for toxicity assessment. *Environ. Res.* 1999; 81(4):259-274. <https://doi.org/10.1006/enrs.1999.3960>
- [48] Seilkop SK, Oller AR. Respiratory cancer risks associated with low-level nickel exposure: An integrated assessment based on animal, epidemiological, and mechanistic data. *Regulatory Toxicology and Pharmacology.* 2003;37(2):173–190. [http://dx.doi.org/10.1016/S0273-2300\(02\)00029-6](http://dx.doi.org/10.1016/S0273-2300(02)00029-6)
- [49] Babai KS, Poongothai S, Lakshmi KS, Punniyakotti J, Meenakshisundaram V. Estimation of indoor radon levels and absorbed dose rates in air for Chennai city, Tamilnadu, India. *Journal of Radioanalytical and Nuclear Chemistry.* 2012; 293(2):649–654. <http://dx.doi.org/10.1007/s10967-012-1718-x>
- [50] Horton RK. An Index Number System for Rating Water Quality. *Journal of the Water Pollution Control Federation.* 1965; 37(3):300-306. [http://www.scirp.org/\(S\(i43dyn45teexjx455qlt3d2q](http://www.scirp.org/(S(i43dyn45teexjx455qlt3d2q)
- [51] Wagh M Vasant, Panaskar Dipak, Aniket AM, Ranjitsinh P. GIS and Statistical Approach to Assess the Groundwater Quality of Nanded Tehsil, (M.S.) India. Springer International Publishing Switzerland 2016. S.C. Satapathy and S. Das (eds.), *Proceedings of First International Conference on Information and Communication Technology for Intelligent Systems: Smart Innovation, Systems and Technologies.* 2016; 50(1):409-417. [http://dx.doi.org/10.1007/978-3-319-30933-0\\_41](http://dx.doi.org/10.1007/978-3-319-30933-0_41)
- [52] Nesrine N, Rachida B, Ahmed R. Multivariate statistical analysis of saline water a case study: Sabkha Oum LeKhialate (Tunisia). *International Journal of Environmental Science Development.* 2015; 6: 40–43. <https://doi.org/10.7763/IJESD.2015.V6.558>
- [53] Rajmohan N. et al. Appraisal of trace metals pollution, sources and associated health risks using the geochemical and multivariate statistical approach, *Appl. Water Sci.* 2023;13(5):113.
- [54] arsimha Adimalla, Sudarshan Venkatayogi. Geochemical characterization and evaluation of groundwater suitability for domestic and agricultural utility in the semi-arid region of Basara, Telangana State, South India. Springer, *Applied Water Science.* 2018; 8:44. <https://doi.org/10.1007/s13201-018-0682-1>
- [55] Lee CSL, Li X Shi, W Cheung SC, Thornton I. Metal contamination in urban, suburban, and country park soils of Hong Kong: a study based on GIS and multivariate statistics. *Science of the Total Environment.* 2006; 356:45–61. <https://doi.org/10.1016/j.scitotenv.2005.03.024>
- [56] Bhuiyan MAH, Parvez L, Islam MA, Dampare SB, Suzuki S. Heavy metal pollution of coal mine-affected agricultural soils in the northern part of Bangladesh. *J. Hazard Mater.* 2011;190 (1–3):876–885.

- [57] Saha N, Rahman MS. Multivariate statistical analysis of metal contamination in surface water around Dhaka export processing industrial zone, Bangladesh. *Environ. Nanotechnol. Monit. Manag.* 2018; 10:206–211. <https://doi.org/10.1016/j.enmm.2018.07.007>
- [58] Indian Standard Specification for Drinking Water, Bureau of Indian Standards, BIS: 10500 (2012) Bureau of Indian Standards Manak Bhawan, New Delhi.